Figures and figure supplements

LRG1 is an adipokine that promotes insulin sensitivity and suppresses inflammation

Chan Hee J Choi *et al*

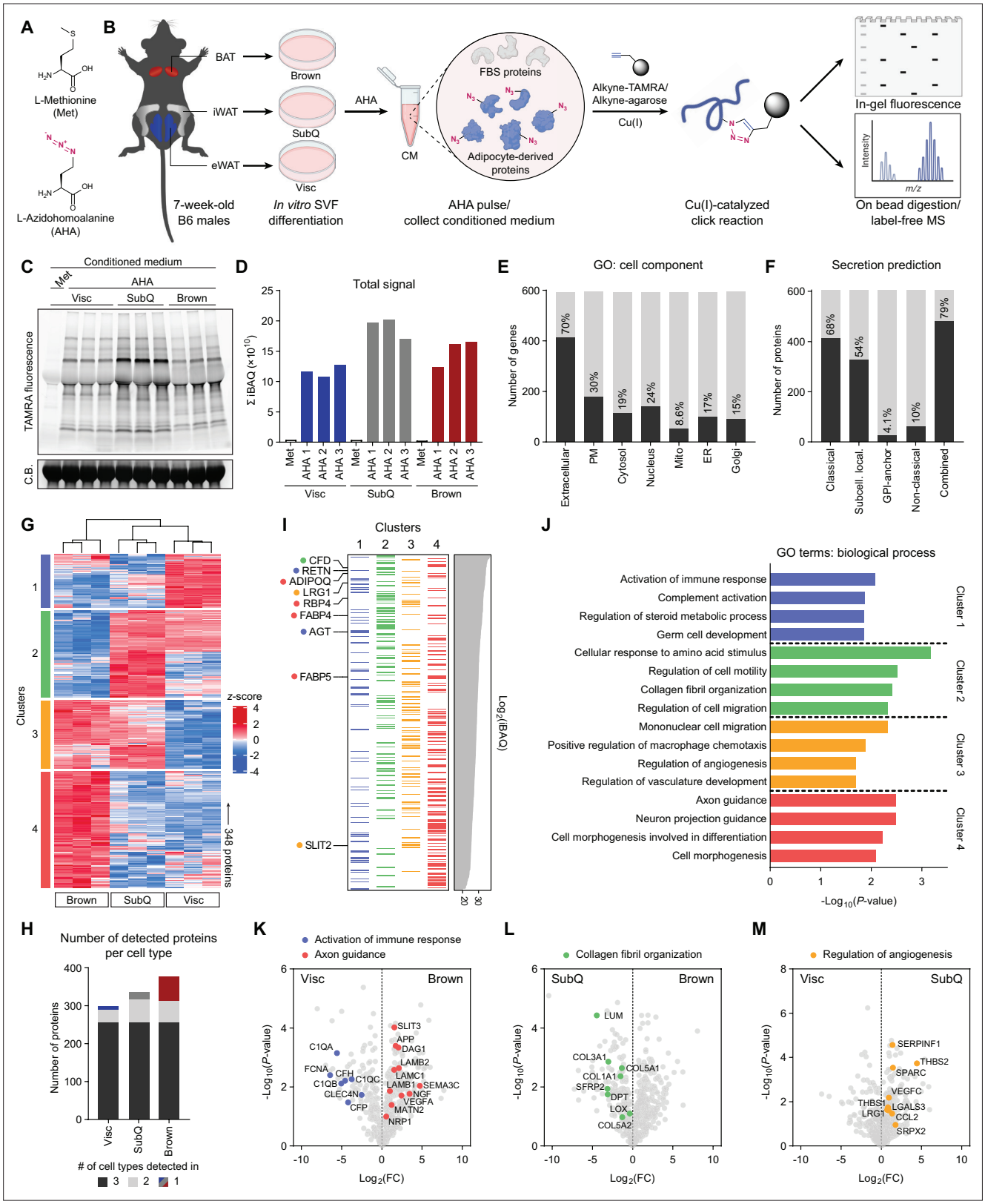


Figure 1. Characterization of primary adipocyte secretome using BONCAT. (**A**) Chemical structures of L-methionine (Met) and L-azidohomoalanine (AHA). (**B**) Schematic diagram of MS-based secretome analysis from primary Visc, SubQ, and Brown adipocytes using BONCAT. (**C**) In-gel fluorescence analysis of TAMRA-conjugated CM proteins from Met-pulsed (lane 1) or AHA-pulsed (lanes 2–10) adipocytes. C.B., Coomassie Blue. (**D**) Sum of iBAQ intensities (Σ iBAQ) across all quantified proteins in each CM. (**E**) Number and proportion of genes annotated to GO cell component terms.

Figure 1 continued on next page

Figure 1 continued

Extracellular, extracellular region, space, or matrix; PM, plasma membrane; Mito, mitochondrion; ER, endoplasmic reticulum; Golgi, Golgi apparatus. (**F**) Number and proportion of proteins predicted to be secreted by prediction algorithms. (**G**) Heatmap of 348 differentially secreted proteins across cell types. (**H**) Number of proteins detected in at least two of three biological replicates per cell type, color-coded based on number of cell types a protein is detected in. (**I**) 348 proteins grouped in clusters from (**G**) and arranged in decreasing order of iBAQ intensities. Previously described adipokines are indicated. (**J**) Top 4 overrepresented GO biological process terms per cluster and their enrichment scores. (**K–M**) Pairwise comparisons of Log_2(LFQ) intensities between Visc and Brown (**K**), SubQ and Brown (**L**), and Visc and SubQ (**M**) CM. Proteins and their annotated pathway terms from (**J**) are indicated.

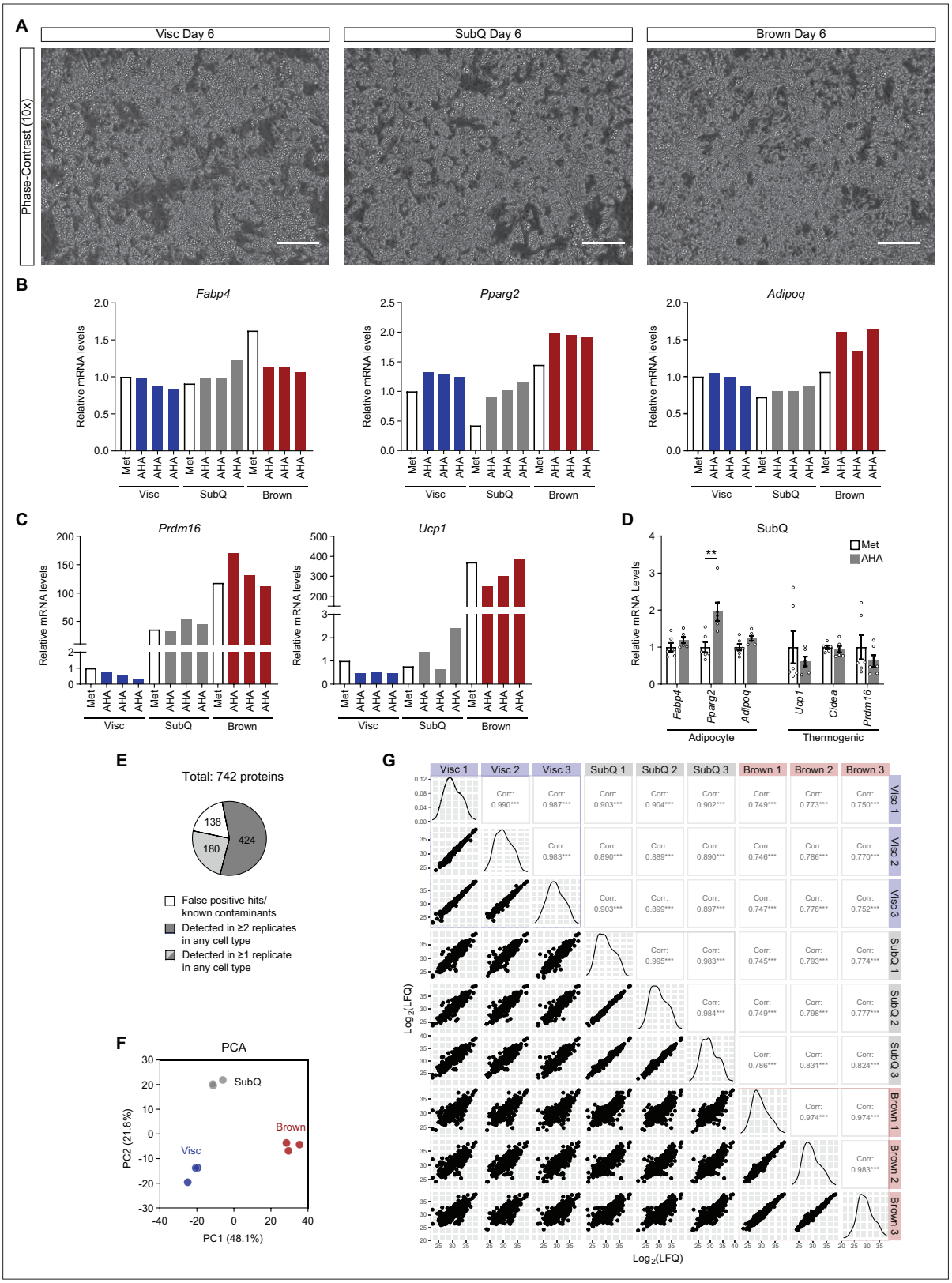


Figure 1—figure supplement 1. Validation of primary adipocyte differentiation and overview of MS results. (**A**) Phase-contrast microscope images of mature Visc, SubQ, and Brown adipocytes on day 6 of differentiation. Scale bars indicate 500 μm. (**B**) Relative mRNA levels of mature adipocyte genes. (**C**) Relative mRNA levels of brown fat-enriched genes, *Prdm16* and *Ucp1*. (**D**) Relative mRNA levels of mature adipocyte and thermogenic genes in primary SubQ adipocytes pulsed with Met of AHA for 24 hr. Data are presented as mean ± SEM. **p<0.01 from two-sided Welch's *t*-test. n=6 technical

Figure 1—figure supplement 1 continued on next page

Figure 1—figure supplement 1 continued

replicates per group. (**E**) Distribution of detected proteins based on exclusion criteria and number of replicates a protein was detected in. (**F**) PCA of AHA-pulsed samples. (**G**) Pairwise comparisons of AHA-pulsed samples. Scatterplot Log_2(LFQ) intensities are displayed on the bottom-left, distribution on the diagonal, and Pearson correlation coefficients on the top-right.

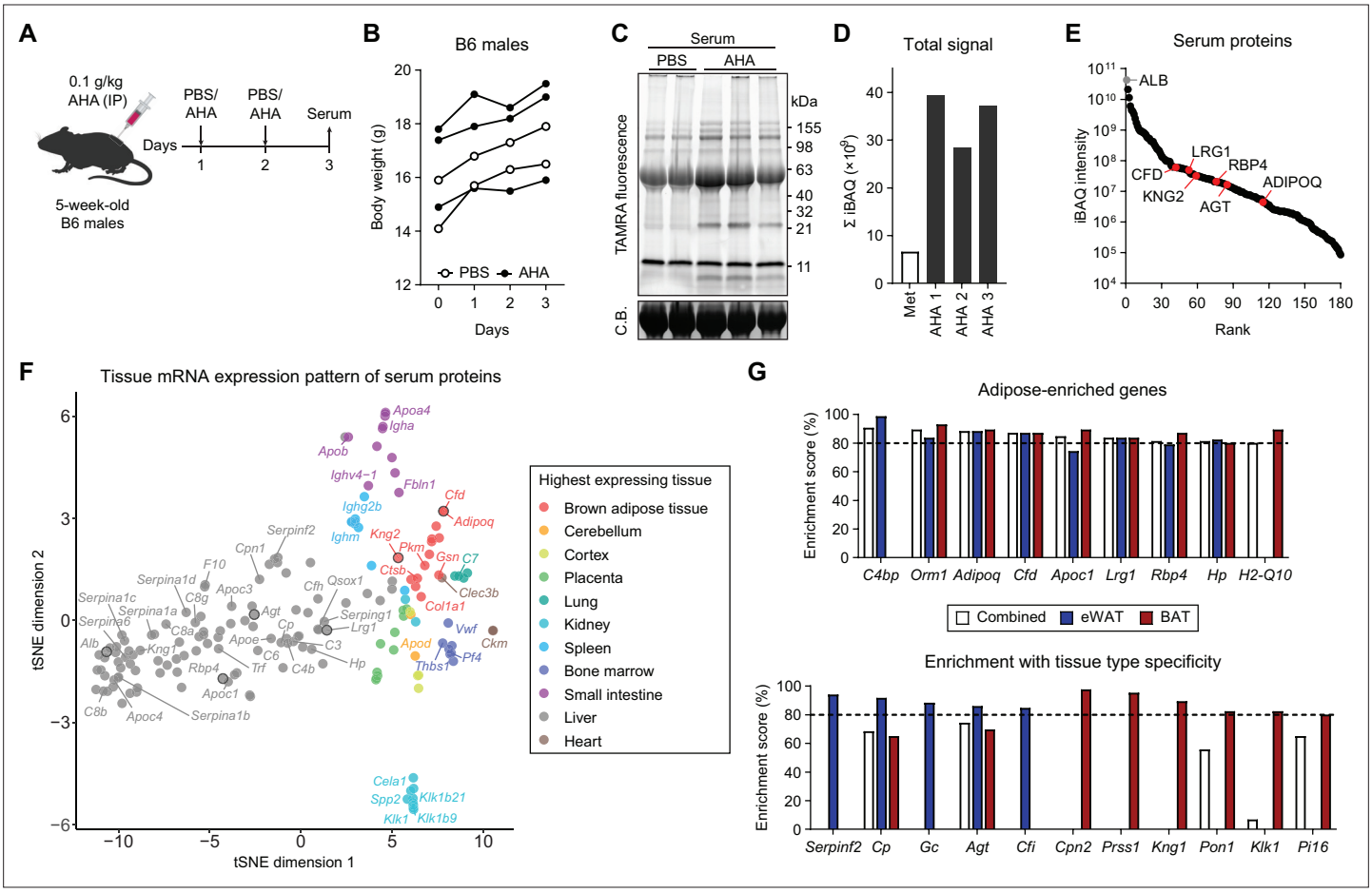


Figure 2. Profiling in vivo nascent serum proteome using BONCAT. (**A**) Schematic of AHA IP injections. (**B**) Body weights of mice injected with PBS (n=2) or AHA (n=3). (**C**) In-gel fluorescence analysis of TAMRA-conjugated serum proteins from PBS-pulsed (lanes 1 and 2) or AHA-pulsed (lanes 3–5) mice. C.B., Coomassie Blue. (**D**) Sum of iBAQ intensities (Σ iBAQ) across all quantified proteins in each serum. (**E**) iBAQ intensities of detected serum samples arranged in decreasing order. (**F**) t-SNE clustering of detected serum protein genes based on tissue mRNA levels from the ENCODE/LICR dataset. (**G**) Adipose tissue-enriched serum protein genes and % enrichment scores calculated from Bio-GPS dataset.

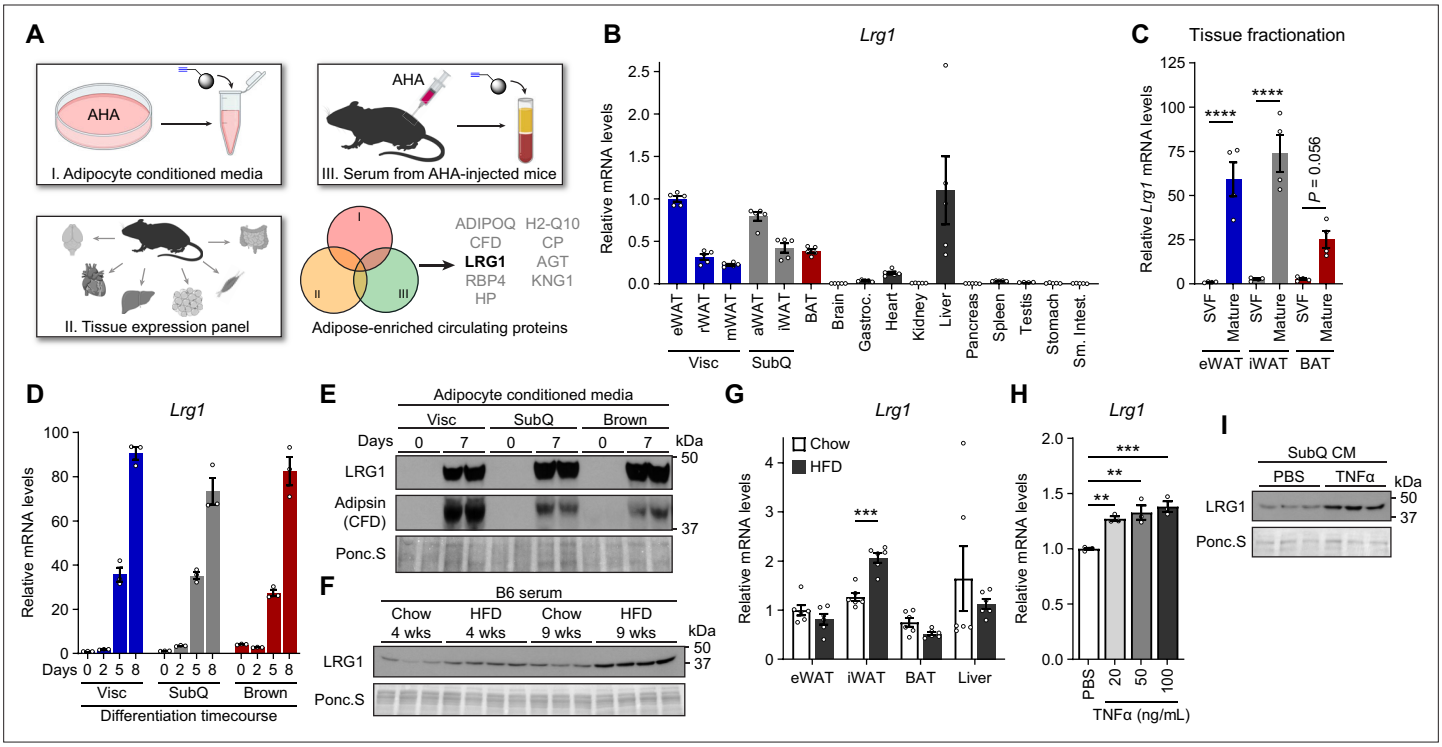


Figure 3. LRG1 is secreted by mature adipocytes and increased in obesity. (**A**) Search strategy for identification of novel adipokines with a potential role in whole-body metabolism. (**B**) Relative *Lrg1* mRNA levels across a panel of tissues from 8-week-old male B6 mice. Visc, visceral fat depots; SubQ, subcutaneous fat depots. n=4–5 biological replicates per group. (**C**) Relative *Lrg1* mRNA levels of indicated adipose tissues fractionated into mature adipocytes and SVF. ****p<0.0001 from Šídák post hoc test following two-way ANOVA. n=4 biological replicates per group. (**D**) Relative *Lrg1* mRNA levels during in vitro differentiation of primary SVF into adipocytes. n=3 technical replicates per group. (**E**) Western blot of LRG1 and CFD in CM before (day 0) and after (day 7) in vitro adipogenic differentiation, in technical replicates. (**F**) Serum western blot of LRG1 from male B6 mice on standard chow or HFD for indicated weeks. HFD was started at 6 weeks of age. Each lane represents a biological replicate. (**G**) Relative *Lrg1* mRNA levels of indicated tissues from mice on standard chow or HFD for 15 weeks. HFD was started at 6 weeks of age. ***p<0.001 from two-sided Welch's *t*-test. n=6 biological replicates per group. (**H**) Relative *Lrg1* mRNA levels of primary SubQ adipocytes treated with recombinant TNFα and 850 nM insulin for 6 hr. **p<0.01, ***p<0.001 from Dunnett post hoc test following one-way ANOVA. n=3 technical replicates per group. (**I**) Western blot of LRG1 in CM of primary SubQ adipocytes treated with PBS or 100 ng/mL recombinant TNFα without insulin for 24 hr. Each lane represents a technical replicate. Data are presented as mean ± SEM.

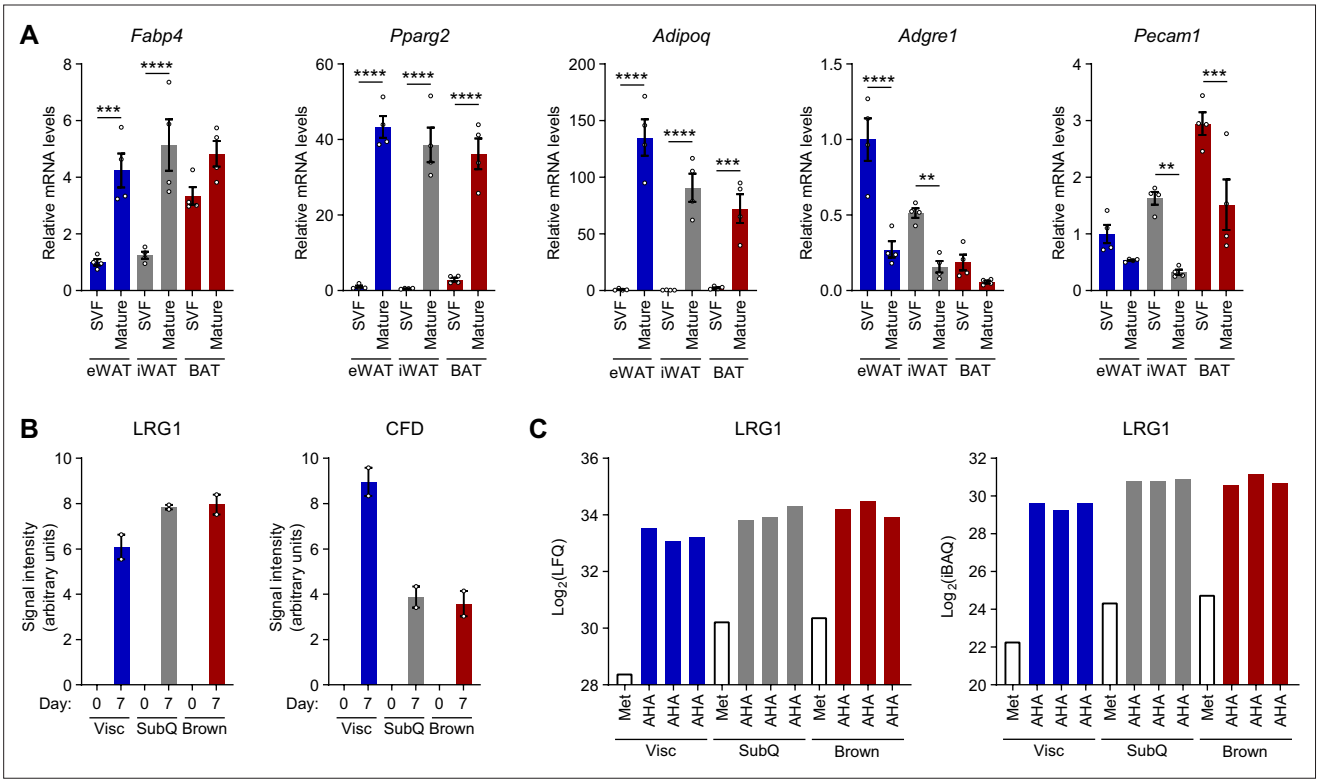


Figure 3—figure supplement 1. Validation of tissue fractionation and quantification of LRG1 in adipocyte CM. (**A**) Relative mRNA levels of mature adipocyte markers, *Fabp4*, *Pparg2*, and *Adipoq* and SVF markers, *Adgre1* and *Pecam1*, in indicated tissues fractionated into mature adipocytes and SVF. Data are presented as mean ± SEM. ***p<0.001, ****p<0.0001 vs. SVF, from Šídák post hoc test following two-way ANOVA. n=4 biological replicates per group. (**B**) Quantification of intensities from ***Figure 3E***. (**C**) LRG1 Log_2(LFQ) and Log_2(iBAQ) intensities detected by MS analysis of alkyne-agarose enriched CM.

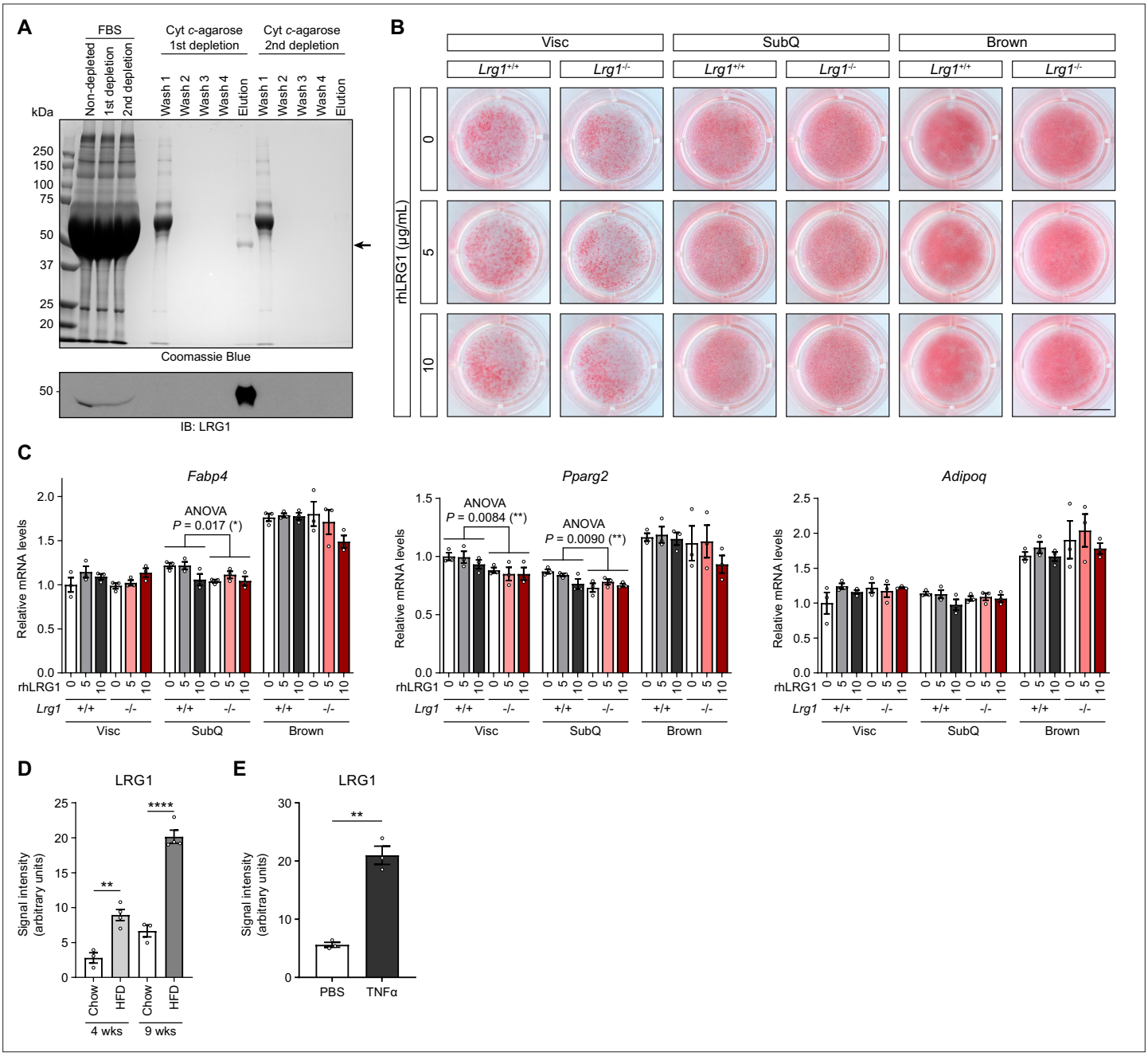


Figure 3—figure supplement 2. LRG1 gain or loss of function does not affect adipogenesis. (**A**) Depletion of bovine LRG1 in FBS using Cyt *c*-conjugated agarose beads. Arrow indicates LRG1. (**B**) Oil red O stain of *Lrg1*$^{+/+}$ or *Lrg1*$^{-/-}$ primary adipocytes treated with indicated concentrations of recombinant human LRG1 (rhLRG1). SVF was grown and differentiated into adipocytes in media containing 10% LRG1-depleted FBS. Scale bar indicates 1 cm. (**C**) Relative mRNA levels of mature adipocyte markers in adipocytes from (**B**). Data are presented as mean ± SEM. ANOVA *P* indicates genotype-factor p-values from two-way ANOVA. *p<0.05, **p<0.01. n=3 technical replicates per group. (**D**) Quantification of intensities from ***Figure 3F***. **p<0.01, ****p<0.0001 from Šídák post hoc test following two-way ANOVA. n=3–4 biological replicates per group. (**E**) Quantification of intensities from ***Figure 3I***. **p<0.01 from two-sided Welch's *t*-test. n=3 technical replicates per group. Data are presented as mean ± SEM.

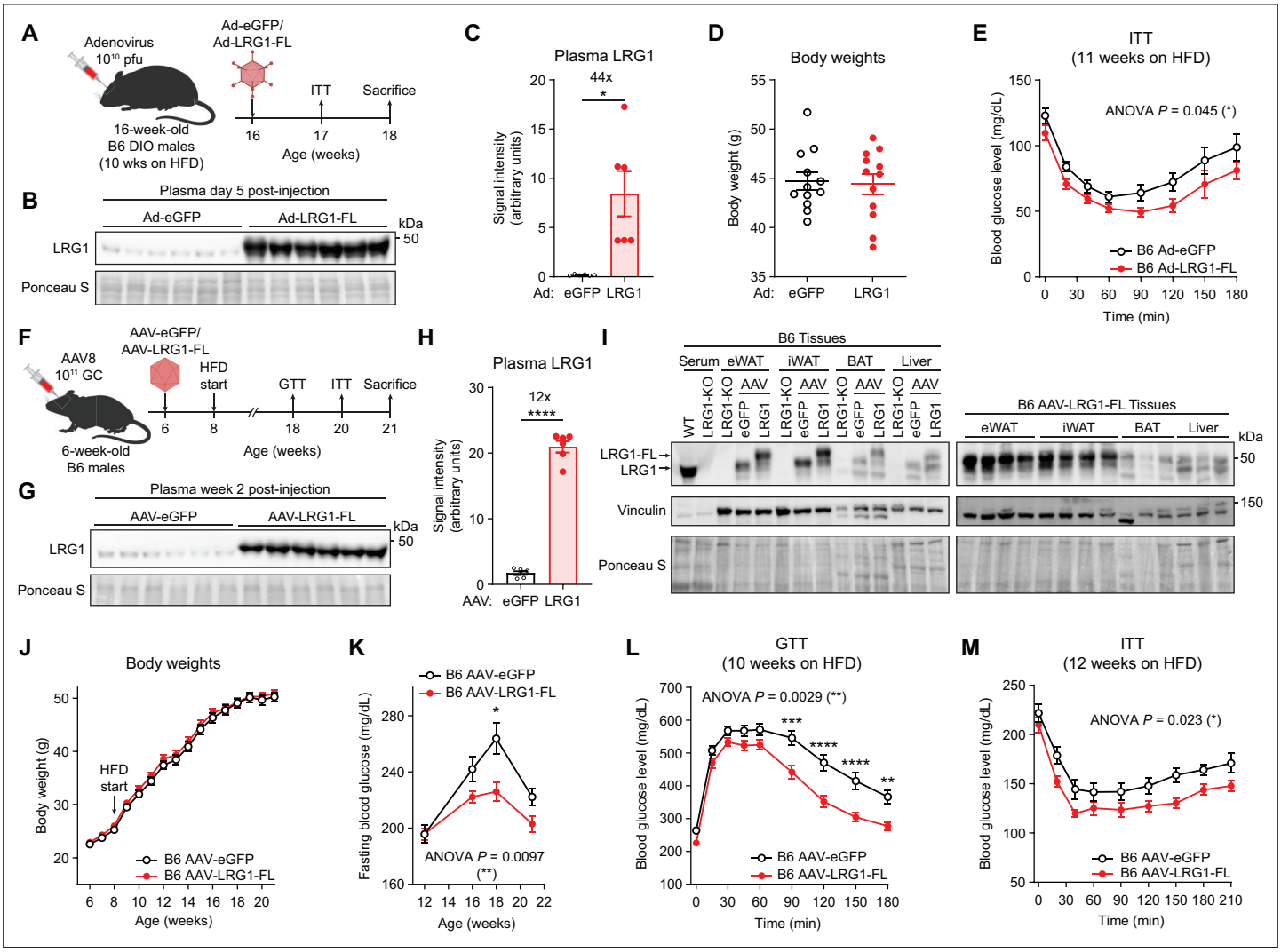


Figure 4. LRG1 overexpression improves glucose homeostasis in C57BL/6 J DIO mice. (**A**) Schematic of Ad vector-mediated acute LRG1 overexpression in B6 DIO male mice. (**B**) Plasma western blot of LRG1 5 days after Ad injection. (**C**) Quantification of (**B**). *p<0.05 from two-sided Welch's *t*-test. n=6 per group. (**D**) Body weights of Ad-transduced B6 males at 17 weeks of age (11 weeks on HFD). (**E**) Insulin tolerance test (1.0 U/kg) in Ad-transduced B6 males at 17 weeks of age (11 weeks on HFD). Ad cohort consisted of n=12 per group. (**F**) Schematic of AAV8-mediated chronic LRG1 overexpression in B6 males. AAV injection was performed in 6-week-old B6 males. HFD was started at 8 weeks of age. (**G**) Plasma western blot of LRG1 2 weeks after AAV injection. (**H**) Quantification of (**G**). ****p<0.0001 from two-sided Welch's *t*-test. n=6 biological replicates per group. (**I**) Left: western blot of LRG1 in serum and tissues from WT vs. LRG1-KO and B6 mice transduced with AAV-eGFP vs. AAV-LRG1-FL. Right: western blot of LRG1 in various tissues from AAV-LRG1-FL-transduced B6 mice. (**J**) Body weights of AAV-transduced B6 male mice during HFD challenge. (**K**) 6 hr fasting blood glucose levels of AAV-transduced B6 male mice during HFD feeding. (**L**) Intraperitoneal glucose tolerance test (1.5 g/kg) in AAV-transduced B6 males at 18 weeks of age (10 weeks on HFD). (**M**) Insulin tolerance test (1.5 U/kg) in AAV-transduced B6 males at 20 weeks of age (12 weeks on HFD). AAV cohort consisted of n=12 per group. Data are presented as mean ± SEM. In (**E, K, L, M**), ANOVA p indicates group factor p-values from repeated measures two-way ANOVA. Where indicated, p-values from Šídák post hoc tests are reported. *p<0.05, **p<0.01, ***p<0.001, ****p<0.0001.

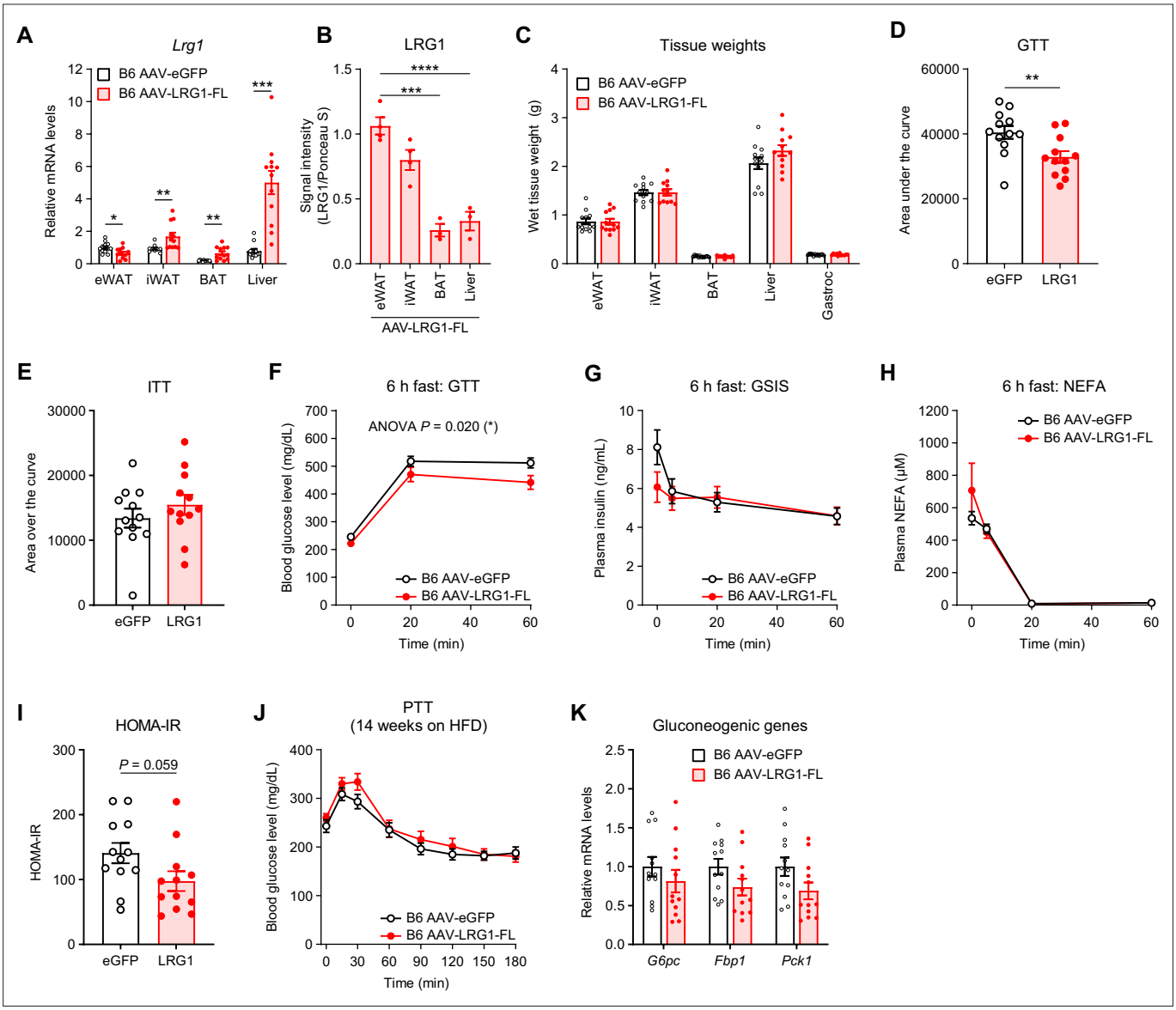


Figure 4—figure supplement 1. Metabolic characterization of AAV-transduced B6 mice. (**A**) Relative *Lrg1* mRNA levels across AAV-transduced B6 males at 21 weeks of age (13 weeks on HFD). *p<0.05, **p<0.01, ***p<0.001 from two-sided Welch's *t*-test. (**B**) Quantification of band intensities from ***Figure 4I***. ***p<0.001, ****p<0.0001 from Tukey post hoc test following one-way ANOVA. n=3–4 biological replicates per group. (**C**) Weights of dissected tissues from AAV-transduced B6 males from (**A**). (**D**) Area under the curve analysis of GTT in ***Figure 4L*** after subtracting baseline measurement at *t*=0. **p<0.01 from two-sided Welch's *t*-test. (**E**) Area over the curve analysis of ITT in ***Figure 4M*** after subtracting baseline measurement at *t*=0. (**F**) Intraperitoneal glucose tolerance test (1.5 g/kg) following a 6 hr fast in AAV-transduced B6 males at 20 weeks of age (12 weeks on HFD). ANOVA *P* indicates group factor p-values from repeated measures two-way ANOVA. (**G**) Plasma insulin levels from (**F**). (**H**) Plasma non-esterified fatty acid (NEFA) levels from (**F**). (**I**) Calculation of HOMA-IR at *t*=0 from (**F**) and (**G**). p-Value from two-sided Welch's *t*-test. (**J**) Oral pyruvate tolerance test (2.0 g/kg) following a 6 h fastr in AAV-transduced B6 males at 22 weeks of age (14 weeks on HFD). (**K**) Relative mRNA levels of gluconeogenic genes in the liver of B6 males at 21 weeks of age (13 weeks on HFD). Data are presented as mean ± SEM. n=12 per group.

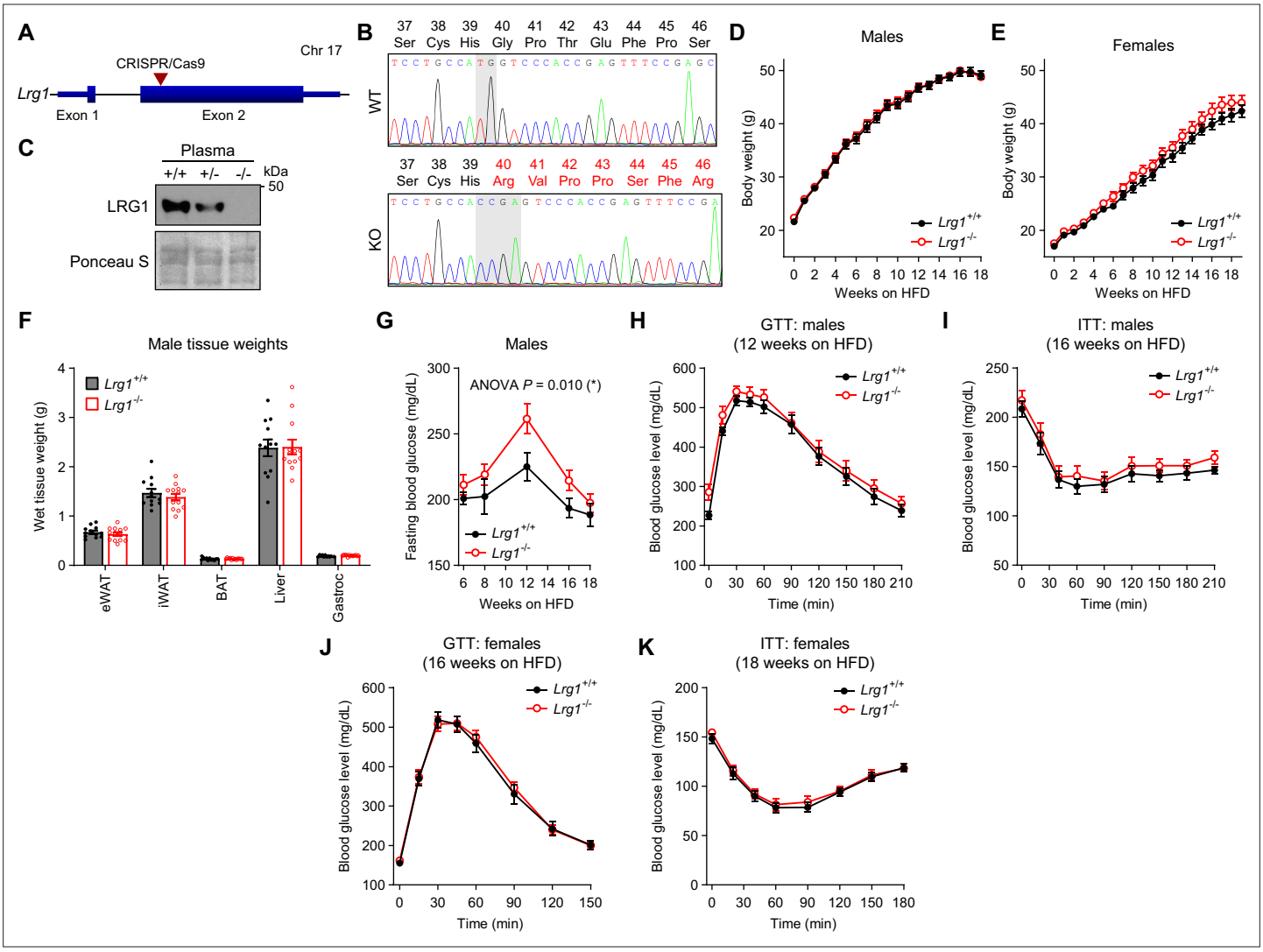


Figure 4—figure supplement 2. LRG1 loss of function in C57BL/6 J DIO mice elevates fasting blood glucose. (**A**) Schematic diagram of murine *Lrg1* exon structure. Red arrowhead indicates the region targeted by CRISPR/Cas9 gRNA. (**B**) Sanger sequencing chromatogram of PCR products amplifying a portion of *Lrg1* exon 2. Shaded portion highlights where sequences differ between WT and LRG1-KO alleles. LRG1 amino acid positions and residues encoded by each allele are indicated above each trace. (**C**) Western blot of LRG1 in plasma of WT (+/+), LRG1-heterozygote (+/-), and LRG1-KO (-/-) mice. (**D**) Body weights of LRG1-KO and WT littermate males on HFD started at 6 weeks of age. (**E**) Body weights of LRG1-KO and WT littermate females on HFD started at 6 weeks of age. (**F**) Dissected tissue weights from LRG1-KO and WT littermate males at 24 weeks of age (18 weeks on HFD). (**G**) 6 hr fasting blood glucose levels of LRG1-KO and WT littermate males during HFD feeding. ANOVA p indicates group factor p-values from repeated measures two-way ANOVA. *p<0.05. (**H**) Intraperitoneal glucose tolerance test (1.5 g/kg) in LRG1-KO and WT littermate male mice performed at 18 weeks of age (12 weeks on HFD). (**I**) Insulin tolerance test (1.5 U/kg) in LRG1-KO and WT littermate male mice performed at 22 weeks of age (16 weeks on HFD). (**J**) Intraperitoneal glucose tolerance test (1.75 g/kg) in LRG1-KO and WT littermate female mice performed at 22 weeks of age (16 weeks on HFD). (**K**) Insulin tolerance test (1.0 U/kg) in LRG1-KO and WT littermate female mice performed at 24 weeks of age (18 weeks on HFD). Data are presented as mean ± SEM. Males: n=12 for WT and n=13 for LRG1-KO. Females: n=12 for WT and n=16 for LRG1-KO.

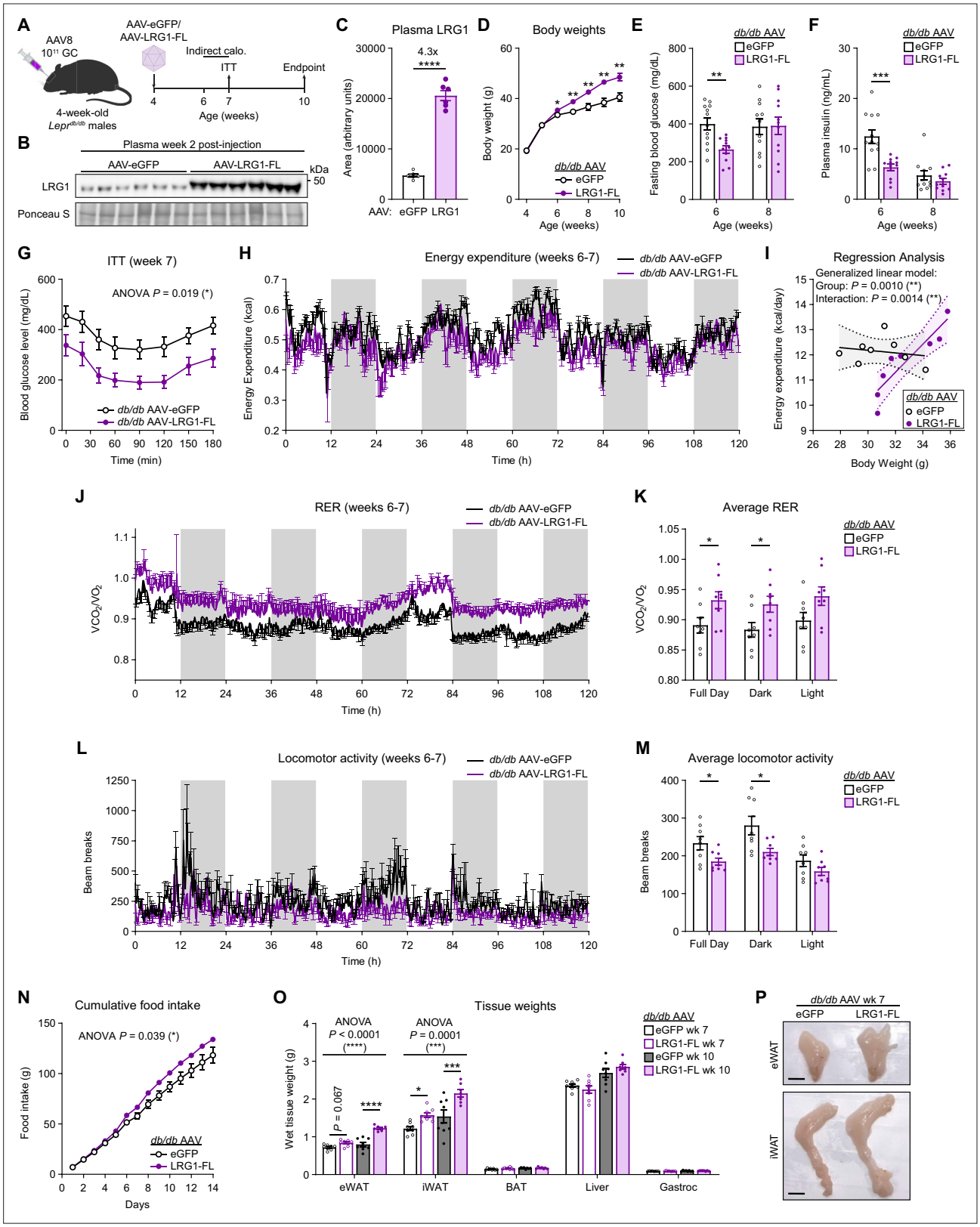


Figure 5. LRG1 overexpression in C57BLKS/J-*Lepr*$^{db/db}$ mice delays onset of diabetic phenotype and promotes WAT expansion. (**A**) Schematic of AAV8-mediated LRG1 overexpression in *db/db* males. (**B**) Plasma western blot of LRG1 2 weeks after AAV injection. (**C**) Quantification of (**B**). ****p<0.0001 from two-sided Welch's *t*-test. n=6 per group. (**D**) Body weights of AAV-transduced *db/db* male mice on standard chow diet. *p<0.05, **p<0.01 from two-sided Welch's *t*-test. n=16 per group for weeks 4–6; n=7–8 per group for weeks 7–10. (**E**) 6 hr fasting blood glucose levels of AAV-transduced *db/db*

Figure 5 continued on next page

Figure 5 continued

male mice at 6 and 8 weeks of age. **p<0.01 from two-sided Welch's *t*-test. n=11–12 per group. (**F**) Plasma insulin levels from (**D**). ***p<0.001 from two-sided Welch's *t*-test. (**G**) Insulin tolerance test (2.0 U/kg) in AAV-transduced 7-week-old *db/db* male mice. ANOVA p indicates group factor p-value from repeated measures two-way ANOVA. *p<0.05. n=7–8 per group. (**H**) Energy expenditure (EE) of AAV-transduced *db/db* male mice measured by indirect calorimetry over the course of 5 days (120 hr). Shaded regions indicate dark cycles. (**I**) Regression analysis of EE vs. body weight from (**H**). (**J**) Respiratory exchange ratio (RER) of AAV-transduced *db/db* male mice in (**H**). (**K**) Daily average of (**J**) *p<0.05 from one-way ANOVA. (**L**) Locomotor activity of AAV-transduced *db/db* male mice in (**H**). (**M**) Daily average of (**L**) *p<0.05 from one-way ANOVA. (**N**) Cumulative daily food intake over the course of 14 days. *p<0.05 from one-way ANOVA. Indirect calorimetry and food intake measurements were performed with n=8 per group. (**O**) Weights of dissected tissues from AAV-transduced *db/db* male mice at 7 and 10 weeks of age. ANOVA p indicates group factor p-values from two-way mixed effects ANOVA. Where indicated, p-values from Šídák post hoc tests reported. *p<0.05, ***p<0.001, ****p<0.0001. n=7–8 per group. (**P**) eWAT and iWAT of AAV-transduced *db/db* male mice at 7 weeks of age. Scale bars indicate 1 cm. Data are presented as mean ± SEM.

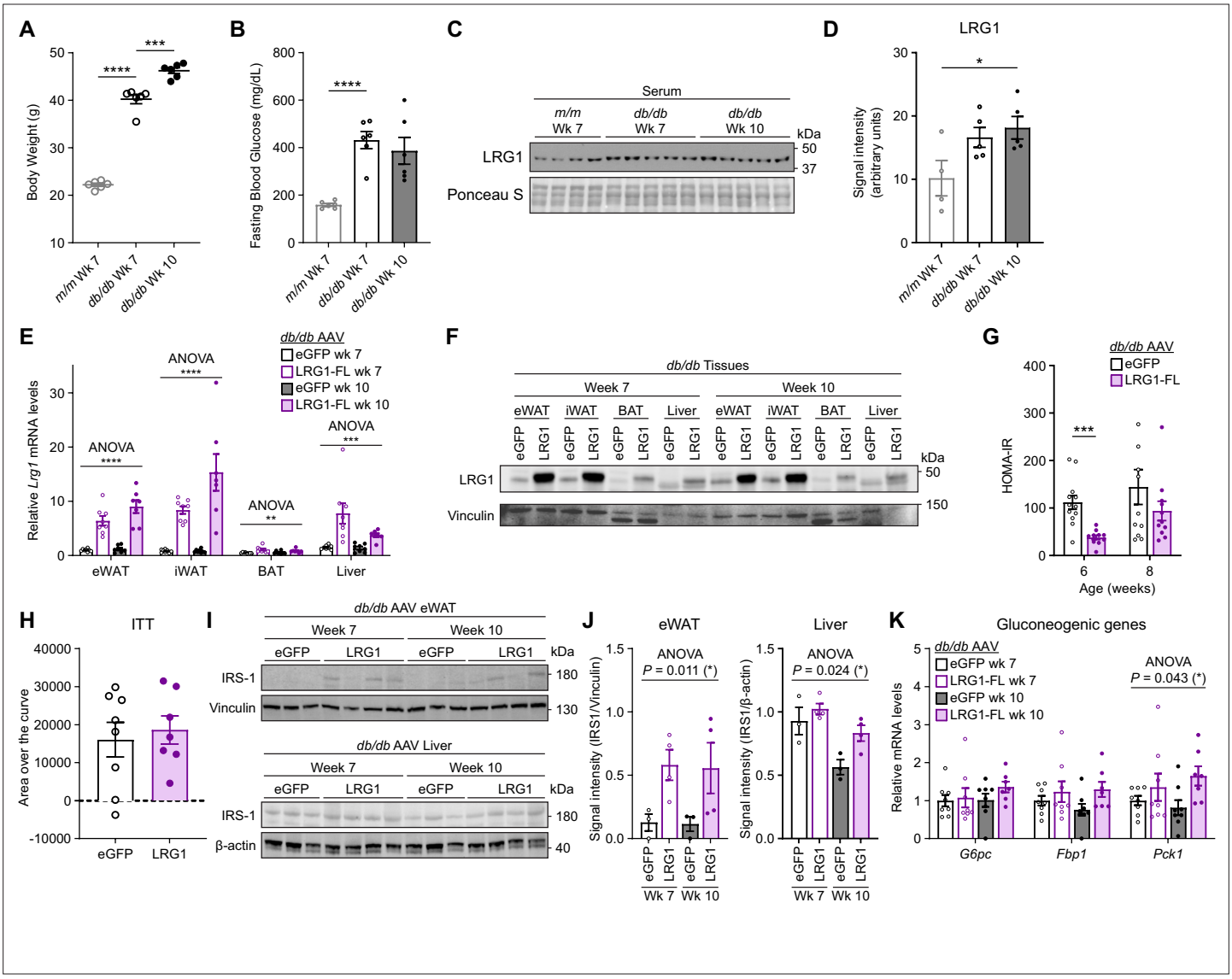


Figure 5—figure supplement 1. Metabolic characterization of *db/db* vs. *m/m* mice and AAV-transduced *db/db* mice. (**A**) Body weights of *db/db* and littermate *m/m* male mice at 7 and 10 weeks of age. ***p<0.001, ****p<0.0001 from two-sided Welch's *t*-test. n=6 per group. (**B**) 6 hr fasting blood glucose levels of *db/db* and littermate *m/m* male mice at 7 and 10 weeks of age. ****p<0.0001 from two-sided Welch's *t*-test. n=6 per group. (**C**) Western blot of LRG1 in serum of *db/db* and littermate *m/m* male mice. (**D**) Quantification of (**C**). *p<0.05 from Tukey post hoc test following one-way ANOVA. (**E**) Relative *Lrg1* mRNA levels across tissues from AAV-transduced *db/db* male mice. **p<0.01, ***p<0.001, ****p<0.0001, group factor significance from two-way ANOVA. n=7–8 per group. (**F**) Western blot of LRG1 in tissues from AAV-transduced *db/db* male mice. (**G**) Calculation of HOMA-IR from ***Figure 5E, F***. ***p<0.001 from two-sided Welch's *t*-test. (**H**) Area over the curve analysis of ITT in ***Figure 5G*** after subtracting baseline measurement at *t*=0. (**I**) Western blot of IRS-1 in eWAT and liver of AAV-transduced *db/db* mice. (**J**) Quantification of (**J**).*p*-value indicates group-factor p-value from two-way ANOVA. n=3–4 biological replicates per group. (**K**) Relative mRNA levels of gluconeogenic genes in the liver of *db/db* males at 7 and 10 weeks of age. *p<0.05 indicates group factor p-value from two-way ANOVA. n=7–8 per group. Data are presented as mean ± SEM.

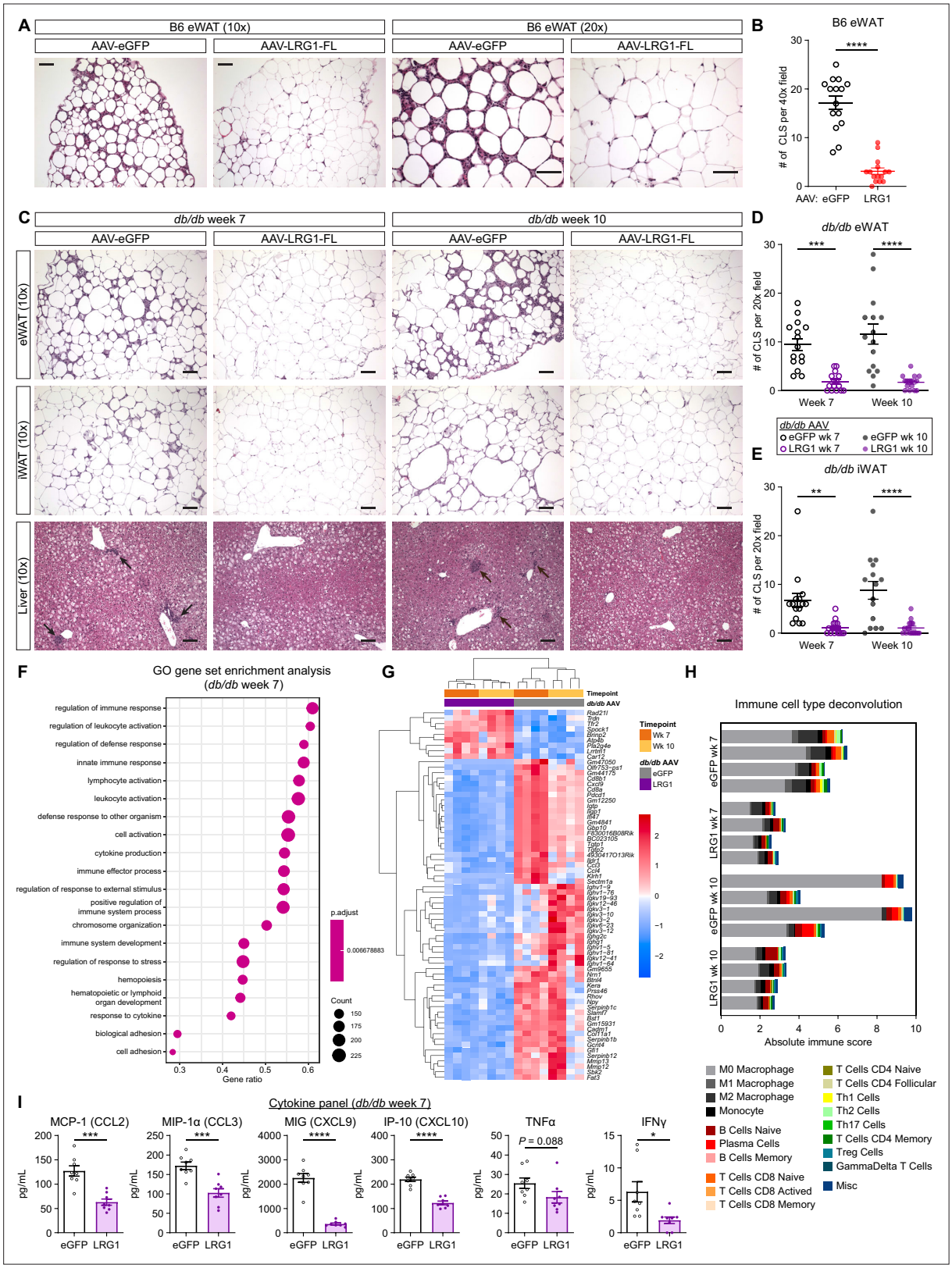


Figure 6. LRG1 suppresses obesity-associated systemic inflammation. (**A**) Representative images from H&E-stained eWAT sections from B6 DIO mice transduced with AAV-eGFP or AAV-LRG1-FL under 10 x (left) and 20 x (right) objectives. Scale bars indicate 100 μm. (**B**) Quantification of CLS from (**A**). ****p<0.0001 from two-sided Welch's *t*-test. 5 fields under a 40 x objective from three animals were used for quantification (n=15 per group). (**C**) Representative images from H&E-stained eWAT, iWAT, and liver sections from *db/db* mice transduced with AAV-eGFP or AAV-LRG1-FL. Arrows indicate

Figure 6 continued on next page

Figure 6 continued

liver inflammatory foci. Scale bars indicate 100 μm. (**D, E**) Quantification of CLS in eWAT (**D**) and iWAT (**E**) from (**C**). Šídák post hoc test results from two-way ANOVA are indicated. **p<0.01, ***p<0.001, ****p<0.0001. Five fields under a 20 x objective from three animals were used for quantification (n=15 per group). (**F**) Top 20 enriched GO BP pathways from GSEA of significantly differentially expressed genes between *db/db*-LRG1 and *db/db*-eGFP eWAT at 7 weeks of age. (**G**) Heatmap of 68 differentially regulated genes (Log_2FC >2 or < –2 and adjusted p<0.01) between *db/db*-LRG1 and *db/db*-eGFP eWAT at both 7 and 10 weeks of age. (**H**) Absolute scores from immune cell type deconvolution analysis of eWAT transcriptomes using CIBERSORTx. (**I**) Quantification of serum chemokine/cytokine levels in *db/db*-LRG1 and *db/db*-eGFP at 7 weeks of age. *p<0.05, ***p<0.001, ****p<0.0001 from two-sided Welch's *t*-test. n=8 biological replicates per group. Data are presented as mean ± SEM.

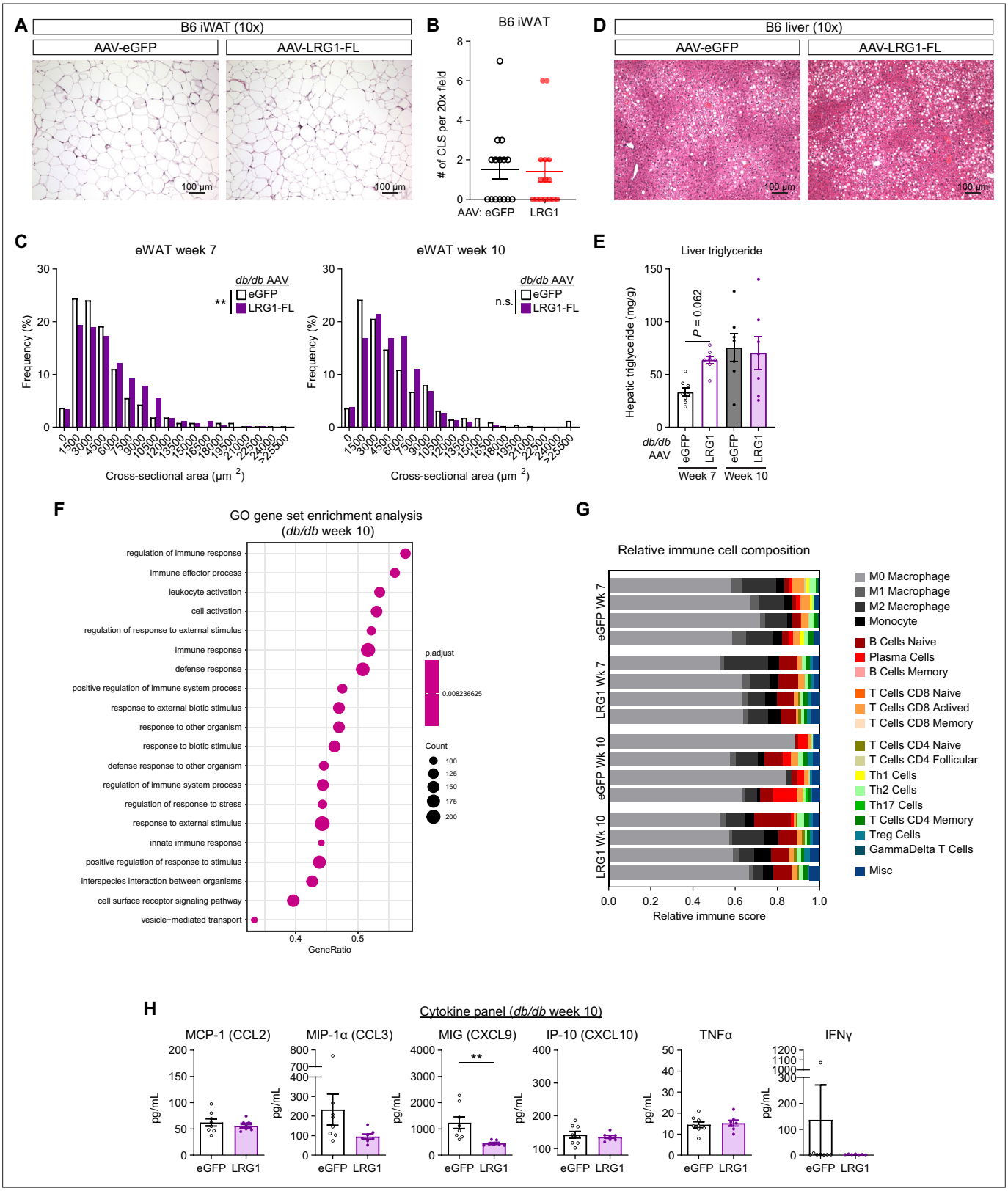


Figure 6—figure supplement 1. Analysis of inflammatory phenotypes with LRG1 gain of function. (**A**) Representative images from H&E-stained iWAT sections from B6 DIO mice transduced with AAV-eGFP or AAV-LRG1-FL. Scale bars are indicated. (**B**) Quantification of CLS from (**A**). Data are presented as mean ± SEM. Five fields under a 20 x objective from three animals were used for quantification (n=15 per group). (**C**) Histogram of adipocyte cross-sectional areas in H&E stained eWAT sections from *db/db*-eGFP and *db/db*-LRG1. **p<0.01 from two-sided Welch's *t*-test. (**D**) Representative images

Figure 6—figure supplement 1 continued on next page

Figure 6—figure supplement 1 continued

from H&E-stained liver sections from B6 DIO mice transduced with AAV-eGFP or AAV-LRG1-FL. Scale bars are indicated. (**E**) Quantification of hepatic triglyceride in *db/db* mice transduced with AAV-eGFP or AAV-LRG1-FL. Data are presented as mean ± SEM. Šídák post hoc test results from two-way ANOVA are indicated. n=7–8 per group. (**F**) Top 20 enriched GO BP pathways from GSEA of significantly differentially expressed genes in eWAT between *db/db*-LRG1 and *db/db*-eGFP at 10 weeks of age. (**G**) Relative scores from immune cell type deconvolution analysis of eWAT transcriptomes using CIBERSORTx. (**H**) Quantification of serum chemokine/cytokine levels in *db/db*-LRG1 and *db/db*-eGFP at 10 weeks of age. Data are presented as mean ± SEM. **p<0.01 from two-sided Welch's *t*-test. n=8 for *db/db*-eGFP and n=7 for *db/db*-LRG1 (biological replicates).

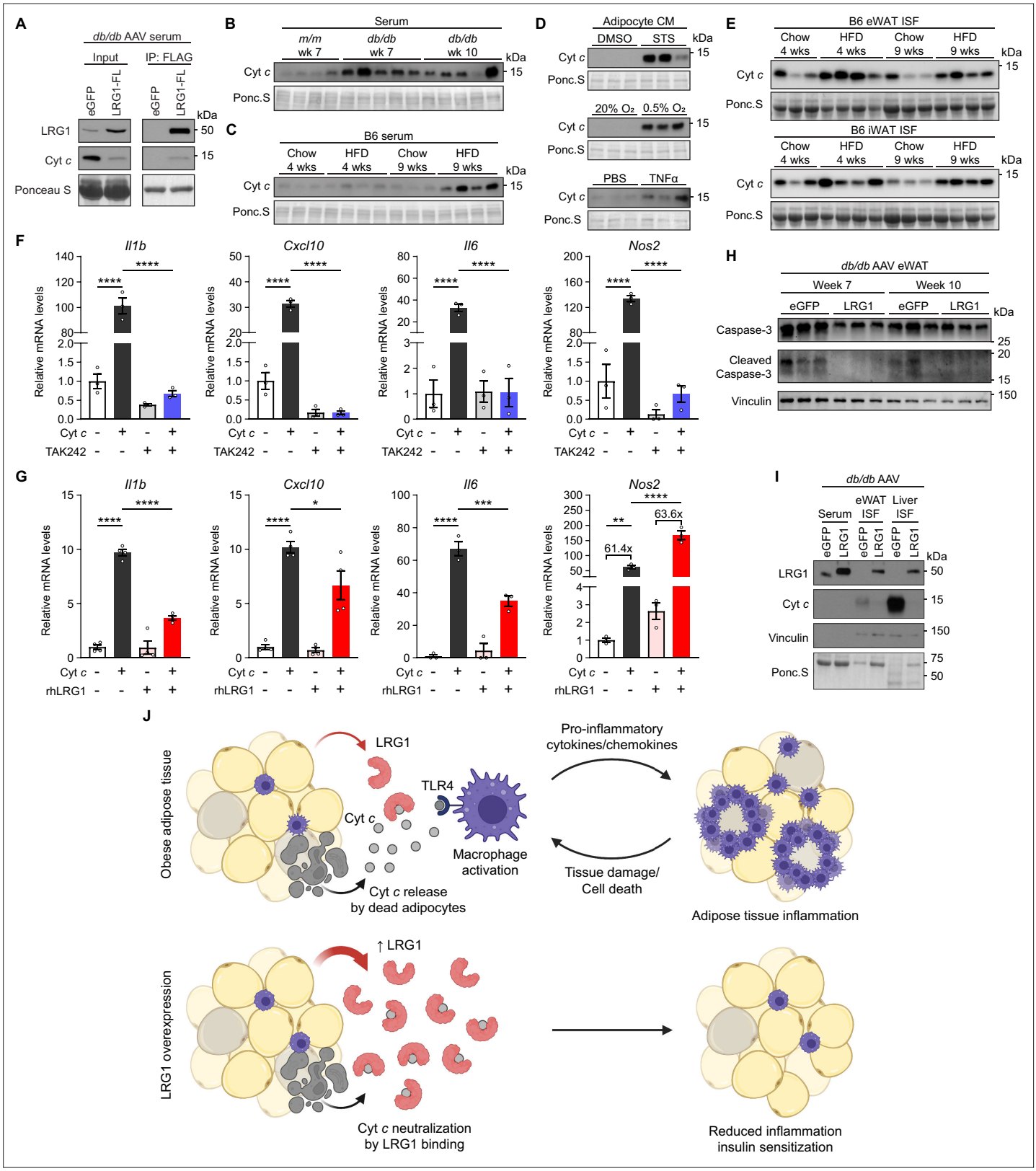
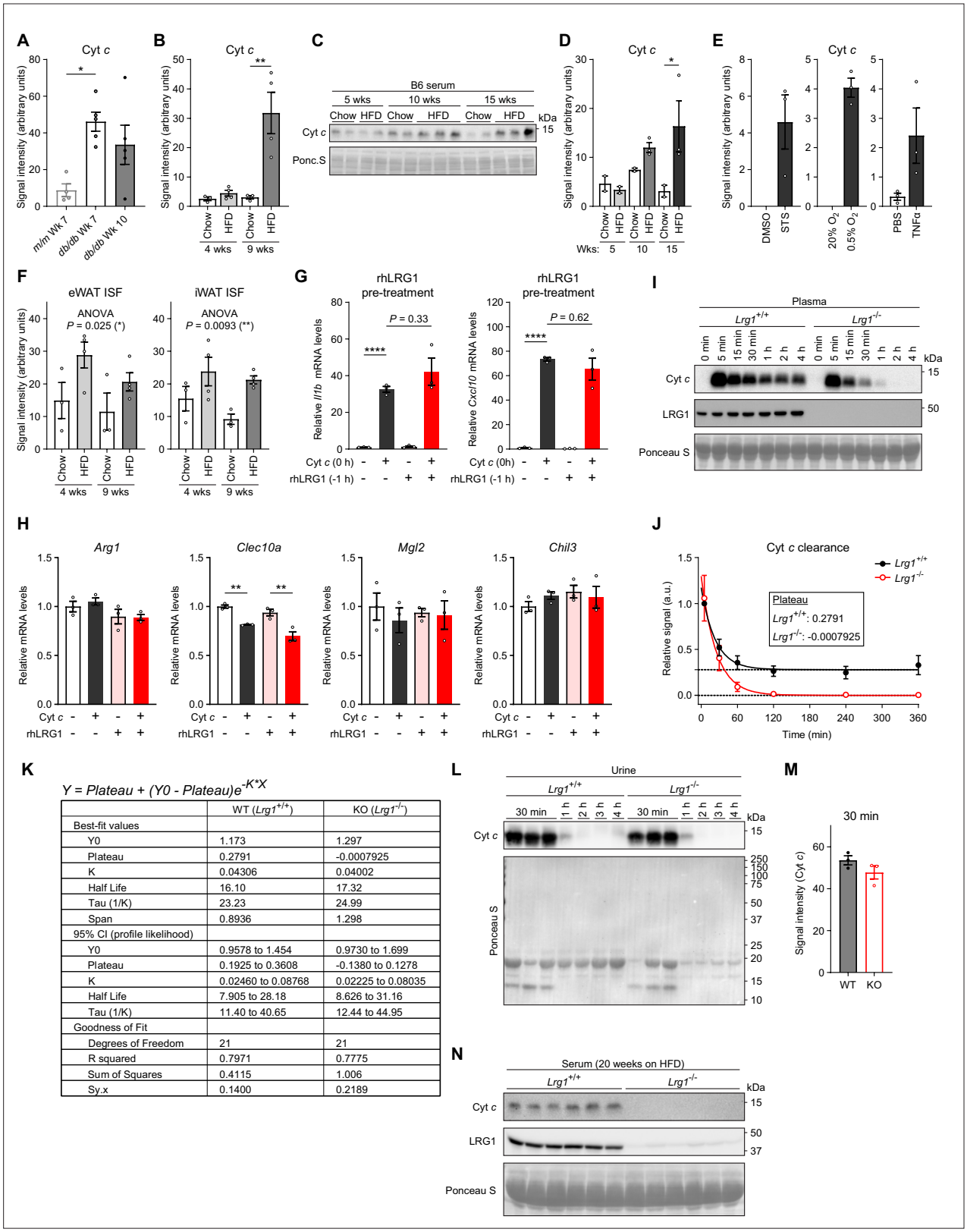


Figure 7. LRG1 binds extracellular cytochrome *c* and blocks its pro-inflammatory effect on macrophages. (**A**) α-FLAG co-IP of C-terminally FLAG-tagged LRG1 and Cyt *c* from the serum of AAV-transduced *db/db* mice at 7 weeks of age. (**B**) Western blot of Cyt *c* in the serum of *db/db* or littermate *m/m* mice at 7 or 10 weeks of age. (**C**) Western blot of Cyt *c* in the serum of B6 mice on standard chow or HFD for indicated weeks. HFD was started at 6 weeks of age. Developed from the same membrane in ***Figure 3F***. (**D**) Western blot of Cyt *c* in the CM of primary SubQ adipocytes under conditions

Figure 7 continued on next page

Figure 7 continued

promoting cell death. SubQ cells were treated with 1 μM staurosporine (STS) or DMSO for 24 hr (top); placed in normoxic or hypoxic chambers for 24 hr (middle); or treated with 100 ng/mL recombinant TNFα or PBS without insulin for 24 hr. Developed from the same membrane in ***Figure 3I*** (bottom). (**E**) Western blot of Cyt *c* in the insterstitial fluid (ISF) of eWAT and iWAT from B6 mice on standard chow or HFD for indicated weeks. (**F**) Relative mRNA levels of a panel of pro-inflammatory genes in BMDMs in response to 30 μg/mL equine Cyt *c* or 10 μM TAK-242, a TLR4 inhibitor. BMDMs were treated with Cyt *c* or PBS for 6 hr following 1 hr pre-incubation with TAK-242 or DMSO. ****p<0.0001 from Tukey post hoc test results following two-way ANOVA. n=3 technical replicates per group. (**G**) Relative mRNA levels of a panel of pro-inflammatory genes in BMDMs in response to 20 μg/mL equine Cyt *c* and 50 μg/mL recombinant human LRG1. Indicated reagents or PBS were rotated for 1 hr at RT prior to BMDM treatment for 6 hr. *p<0.05, **p<0.01, ***p<0.001, ****p<0.0001 from Tukey post hoc test results following two-way ANOVA. n=3–4 technical replicates per group. (**H**) Western blot of intact and cleaved Caspase-3 in eWAT of AAV-transduced *db/db* mice. (**I**) Western blot of LRG1 and Cyt *c* in the serum and ISF of *db/db* mice at 10 weeks of age. Vinculin was used to assess tissue leakage during sample preparation. (**J**) Schematic depicting proposed mechanism. Data are presented as mean ± SEM.



	WT ($Lrg1^{+/+}$)	KO ($Lrg1^{-/-}$)
Best-fit values		
Y0	1.173	1.297
Plateau	0.2791	-0.0007925
K	0.04306	0.04002
Half Life	16.10	17.32
Tau (1/K)	23.23	24.99
Span	0.8936	1.298
95% CI (profile likelihood)		
Y0	0.9578 to 1.454	0.9730 to 1.699
Plateau	0.1925 to 0.3608	-0.1380 to 0.1278
K	0.02460 to 0.08768	0.02225 to 0.08035
Half Life	7.905 to 28.18	8.626 to 31.16
Tau (1/K)	11.40 to 40.65	12.44 to 44.95
Goodness of Fit		
Degrees of Freedom	21	21
R squared	0.7971	0.7775
Sum of Squares	0.4115	1.006
Sy.x	0.1400	0.2189

Figure 7—figure supplement 1. Analysis of LRG1-Cyt *c* interaction. (**A**) Quantification of ***Figure 7B***. *p<0.05 from Tukey post hoc test following one-way ANOVA. n=4–5 biological replicates per group. (**B**) Quantification of ***Figure 7C***. **p<0.01 from Šídák post hoc test following two-way ANOVA. n=3–4 biological replicates per group. (**C**) Western blot of Cyt *c* in serum of B6 mice on HFD. (**D**) Quantification of (**C**). *p<0.05 from Šídák post hoc test following two-way ANOVA. n=2–3 biological replicates per group. (**E**) Quantification of ***Figure 7D***. n=3 technical replicates per group. (**F**) Quantification

Figure 7—figure supplement 1 continued on next page

Figure 7—figure supplement 1 continued

of ***Figure 7E***. *p<0.05 indicates group factor p-value from two-way ANOVA. n=3–4 biological replicates per group. (**G**) Relative *Il1b* and *Cxcl10* mRNA levels in BMDMs in response to 20 µg/mL equine Cyt *c* with or without 1 hr pre-treatment of 50 µg/mL recombinant human LRG1. Tukey post hoc test results from two-way ANOVA are indicated. ****p<0.0001. n=3 technical replicates per group. (**H**) Relative mRNA levels of a panel of alternatively activated (**M2**) macrophage markers in BMDMs in response to 20 µg/mL equine Cyt *c* and 50 µg/mL recombinant human LRG1. **p<0.01 from Tukey post hoc test following two-way ANOVA. n=3 technical replicates per group. (**I**) Representative western blot of Cyt *c* in plasma of LRG1-KO and WT littermate male mice following retroorbital injection of 40 mg/kg equine Cyt *c*. (**J**) Relative quantification of Cyt *c* intensities from (**I**). Fitted one-phase decay curves and estimated values for the plateau are shown. n=4 biological replicates per group. (**K**) Table summarizing results from least squares regression fit of relative Cyt *c* intensities with one-phase decay functions. (**L**) Urine Cyt *c* western blot and Ponceau S stain of urinary proteins from animals in (**J**). (**M**) Quantification of (**L**). (**N**) Western blot of Cyt *c* in serum of LRG1-KO and WT littermate male mice on HFD for 20 weeks. Data are presented as mean ± SEM.